Part IV

Viscous Dissipation in Porous Media

9

Effect of Viscous Dissipation on the Flow in Fluid Saturated Porous Media

E. Magyari, D.A.S. Rees, and B. Keller

CONTENTS

9.1 Introduction

The viscous dissipation effect, which is a local production of thermal energy through the mechanism of viscous stresses, is a ubiquitous phenomenon and it is encountered in both the viscous flow of clear fluids and the fluid flow within porous media. When compared with other thermal influences on fluid motion (i.e., by means of buoyancy forces induced by heated or cooled walls, and by localized heat sources or sinks) the effect of the heat released by viscous dissipation covers a wide range of magnitudes from being negligible to being significant. Gebhart [1] discussed this range at length and stated that "a significant viscous dissipation may occur in natural convection in various devices which are subject to large decelerations or which operate at high rotational speeds. In addition, important viscous dissipation effects may also be present in stronger gravitational fields and in processes wherein the scale of the process is very large, e.g., on larger planets, in large masses of gas in space, and in geological processes in fluids internal to various bodies." In contrast to such situations, many free convection processes are not sufficiently vigorous to result in a significant quantitative effect, although viscous dissipation sometimes serves to alter the qualitative nature of the flow.

Although viscous dissipation is generally regarded as a weak effect, a property it shares with relativistic and quantum mechanical effects in everyday life, it too has played a seminal role in history of physics. It was precisely this "weak" physical effect that allowed James Prescott Joule in 1843 to determine the mechanical equivalent of heat using his celebrated paddle-wheel experiments, and thereby to set in place one of the most important milestones toward the formulation of the first principle of thermodynamics. Curiously enough, the Royal Society declined to publish Joule's work in the famous *Transactions* (the *Physical Review Letters* of that time) and thus the paper appeared only two years later in a more liberal journal, the *Philosophical Magazine*. Today, papers on viscous dissipation frequently suffer a similar fate as Joule's first paper, and it is often neglected. One of the aims of the present review is to assess the quantitative and qualitative changes brought about by the presence of viscous dissipation.

From a mathematical point of view the effect of viscous dissipation arises as an additional term in the energy equation. It expresses the rate of volumetric heat generation, q''', by internal friction in the presence of a fluid flow. For a plane boundary-layer flow or a unidirectional flow, q''' takes the following forms for clear fluids and for Darcy flow through a porous medium,

$$q'''_{\text{clear}} \equiv \mu \left(\frac{\partial u}{\partial y}\right)^2 \quad \text{and} \quad q'''_{\text{Darcy}} \equiv \frac{\mu}{K} u^2 \tag{9.1a,b}$$

respectively, where μ is the dynamic viscosity and K is the permeability. It would appear that the above expression for q'''_{Darcy} was deduced for the first

time by Ene and Sanchez-Palencia [2] and Bejan [3] in independent works. Other early applications of this "u^2-model" for viscous dissipation in porous media are those of Nakayama and Pop [4], which discusses the external free convection from nonisothermal bodies, and of Ingham et al. [5], which deals with the mixed convection problem between two vertical walls.

From a physical point of view, the difference between the two expressions in Eqs. (9.1a) and (9.1b) originates from the fact that u denotes the actual fluid velocity for a clear fluid flow, but denotes the fluid seepage velocity (i.e., the bulk velocity divided by porosity) for a porous medium flow. At microscopic levels within a porous medium, the fluid is "extruded" through the pores of the solid matrix, and local flows are typically three dimensional even though the overall macroscopic flow is uniform and unidirectional. This microscopic process considerably enhances the rate of heat generation by viscous dissipation. Thus, as can be seen immediately for uniform forced convection flows in clear fluids ($u = \text{const.} \equiv u_\infty$), no heat is released by viscous dissipation, at least by the agency of internal frictional forces. However, in porous media the heat generation rate increases quadratically with u. In the context of boundary-layer flows it has been shown recently [6] that this fact has important consequences for far-field thermal boundary conditions for both forced and mixed convection in extended porous media. For free convection boundary-layer flows, expressions (9.1a) and (9.1b) are both compatible with the uniform asymptotic condition for the temperature, that is, $T(x, y \to \infty) = \text{const.} = T_\infty$. This condition is usually imposed on the temperature field since $u \to 0$ as $y \to \infty$. But in forced and mixed convection flows in extended porous media, this asymptotic thermal condition contradicts the corresponding energy equation because the term $q'''_{\text{Darcy}} = (\mu/K)u_\infty^2$ is nonvanishing as $y \to \infty$. Accordingly, some recent results pertaining to mixed convection flows in extended porous media [7,8] should be reconsidered (see Magyari et al. [9] and responses by Tashtoush [10] and Nield [11]) by taking into account suitably modified boundary conditions on T in the far field ([6] and Sections 9.4 and 9.5).

Even if the quantitative effect of viscous dissipation is negligible in some cases (see exceptions cited by Gebhart [1], Gebhart and Mollendorf [12], and Nield [13], which include situations where high accelerations exist such as in rapidly rotating systems) its qualitative effect may become significant. One interesting effect of the presence of viscous dissipation, to be discussed in more detail later, is the breaking of both the physical and mathematical equivalence that usually exists between a free convective boundary-layer flow ascending from a hot plate ($T_\text{w} > T_\infty$) and its counterpart, descending from a cold plate ($T_\text{w} < T_\infty$). For the latter case the resulting flow is strictly a parallel boundary-layer flow of constant thickness, which has been named the "asymptotic dissipation profile" or ADP (see Magyari and Keller [14] and Section 9.3). A second qualitative difference arises when viscous dissipation is included in a stability analysis of the Darcy–Benard problem — a porous layer heated from below. For a Boussinesq fluid in a Darcian medium with uniform steady temperatures on the boundaries, the basic no-flow state is

first destabilized by two-dimensional roll patterns. The presence of viscous dissipation causes a hexagonal pattern to appear at Rayleigh numbers close to the critical value (see Rees et al. [15]).

This chapter begins with a presentation of the precise mathematical formulae to be used for modeling viscous dissipation, with an emphasis on the very recent debate on the correct form to use when the Brinkman terms are significant in the momentum equations. This is followed by an overview of the current state of the art in free, mixed, and forced convective boundary-layer flows, and some first tentative steps toward the application of stability theory to certain free convective flows.

9.2 Basic Thermal Energy Equations

The thermal energy equation for steady convection in a porous medium may be stated as:

$$\rho c_{\mathrm{p}} \underline{v} \cdot \nabla T = \nabla \cdot (k \nabla T) + \Phi \tag{9.2}$$

where ρ is the density of the saturating fluid, c_{p} its specific heat, and k the thermal conductivity of the saturated porous medium. In Eq. (9.2) it is also assumed that the fluid and the porous material are in local thermal equilibrium. The last term Φ in (9.2) is the viscous dissipation term, previously denoted by q'''_{Darcy}. The purpose of this section is to present the various forms that this term may take when the momentum equations are modeled in different ways.

9.2.1 Darcy Terms

When the flow in an isotropic porous medium satisfies Darcy's law, the appropriate heat-source term that models viscous dissipation in the thermal energy equation is given by (9.1), but only when the flow is undirectional, or when it is predominantly in one direction, such as in a boundary-layer flow. More generally, the full expression for Φ is

$$\Phi = \frac{\mu}{K}(u^2 + v^2 + w^2) \tag{9.3}$$

This form should be used for isotropic media and is independent of the orientation of the coordinate axes. Nield [16] has stated that this form for Φ is obtained by taking

$$\Phi = \underline{v} \cdot \underline{F} \tag{9.4}$$

where $\underline{F}$ is the drag force on the porous medium. Thus, if Darcy's law is valid and the permeability is isotropic, then $\underline{F} = (\mu/K)\underline{v}$. If the drag force argument is used in such circumstances where the porous medium is anisotropic with permeability tensor, $\underline{\underline{K}}$, then (9.3) may be replaced by

$$\Phi = \mu \underline{v} \cdot \underline{\underline{K}}^{-1} \cdot \underline{v} \tag{9.5}$$

9.2.2 Forchheimer Terms

When the microscopic Reynolds number is approximately greater than unity, then the momentum equation is usually supplemented by a quadratic nonlinear term corresponding to form drag within the medium, and the extra term is known as the Forchheimer term. Initially it was thought that the presence of form drag does not affect viscous dissipation because the coefficient of $|\underline{v}|\underline{v}$, which is $c_{fp}K^{-1/2}$, does not involve viscosity [17]. (Here, the value c_{fp} is a nondimensional parameter that is dependent on the geometry of the porous medium.) Recently, Nield [16] used the drag force argument to state that Eq. (9.3) should now read

$$\Phi = \frac{\mu}{K}\underline{v} \cdot \underline{v} + \frac{c_f \rho}{K^{1/2}}|\underline{v}|\underline{v} \cdot \underline{v} \tag{9.6}$$

AQ: Please clarify if the term in eq. (9.6) should be c_{fp}

The apparent paradox that a term that is independent of the viscosity may contribute to the viscous dissipation was resolved in an earlier paper by Nield [13]. Under such conditions, the advective inertia terms in the Navier–Stokes equations are not negligible and therefore wake formation and boundary-layer separation takes place at pore/particle length-scales. This, in turn, means that microscopic velocities are altered and thereby the heat generated by viscous dissipation is increased.

Other versions of the momentum equation exist that have cubic terms; see, for example, Mei and Auriault [18] and Lage et al. [19]. To date such terms have not been included in the expression for Φ using (9.4).

9.2.3 Brinkman Terms

While the form for Φ that is given by (9.6) is widely accepted for Darcy–Forchheimer flow, the same cannot be said for flows where boundary effects, as modeled by the Brinkman terms, are significant. Nield's [16] drag force formula yields the form

$$\Phi = \frac{\mu}{K}\underline{v} \cdot \underline{v} - \tilde{\mu}\underline{v} \cdot \nabla^2 \underline{v} \tag{9.7}$$

where $\tilde{\mu}$ is an effective viscosity, while Al-Hadhrami et al. [20] use an argument based on the work done by frictional forces to obtain,

$$\Phi = \frac{\mu}{K}(u^2+v^2+w^2) + \tilde{\mu}\left[2\left(\frac{\partial u}{\partial x}\right)^2 + 2\left(\frac{\partial v}{\partial y}\right)^2 + 2\left(\frac{\partial w}{\partial z}\right)^2 + \left(\frac{\partial u}{\partial y}+\frac{\partial v}{\partial x}\right)^2 + \left(\frac{\partial u}{\partial z}+\frac{\partial w}{\partial x}\right)^2 + \left(\frac{\partial v}{\partial z}+\frac{\partial w}{\partial y}\right)^2\right] \tag{9.8}$$

Both formulae yield the correct form for Φ in the limit of small permeability, but when the porosity increases toward unity then only the formula of Al-Hadhrami et al. [20] matches that for a clear fluid. While Al-Hadhrami et al. [20] argue further that Nield's [13] formula can in some circumstances yield negative values for Φ, which is physically unacceptable, Nield [16] has countered by questioning the use of the stress tensor in an identical manner to the way it is used in clear fluids. Moreover, he also questions the often indiscriminate use of the Brinkman term, even though it appears to give a smooth transition between Darcy flow and the flow of a clear fluid. However, both Al-Hadhrami et al. [20] and Nield [16] agree that further studies in this area are essential to resolve the present conflict.

9.2.4 Order-of-Magnitude Estimates

Here, we repeat Nield's [13] analysis of the situations in which one might expect viscous dissipation to be significant. This is done by simply comparing the orders of magnitude of the dissipation terms with the thermal diffusion terms in the thermal energy equation. We concentrate on the form of Φ corresponding to Darcy's law, as given in (9.3).

If the quantities, U, L, and ΔT are used to denote representative values of velocity, length, and temperature drop within a system, then the orders of magnitude of the thermal diffusion and viscous dissipation terms in (9.3) are, respectively,

$$\frac{k\Delta T}{L^2} \quad \text{and} \quad \frac{\mu U^2}{K} \tag{9.9}$$

In mixed and forced convective flows there exists a given velocity scale, and therefore viscous dissipation effects are negligible when

$$\left(\frac{\mu U^2}{k\Delta T}\right)\frac{L^2}{K} = \frac{Br}{Da} \ll 1 \tag{9.10}$$

Here *Br* and *Da* are the Brinkman and Darcy numbers where the Brinkman number is the term in brackets in (9.10).

On the other hand, there is no natural length-scale in free convection, but a simple scaling analysis (or even a full vertical thermal boundary-layer analysis along the lines of that undertaken by Cheng and Minkowycz [21]) yields the velocity scale,

$$U \propto \left(\frac{\alpha}{L}\right) Ra^{1/2} \tag{9.11}$$

where

$$Ra = \frac{\rho g \beta K L \Delta T}{\alpha \mu} \quad \text{and} \quad \alpha = k/\rho c_{\mathrm{p}} \tag{9.12}$$

are the Darcy–Rayleigh number and the thermal diffusivity of the medium, respectively. Substitution of the above expression for U into (9.10) yields

$$Ge = \frac{g\beta L}{c_{\mathrm{p}}} \ll 1 \tag{9.13}$$

as the condition for viscous dissipation to be negligible. The quantity *Ge* is the Gebhart number.

Given the forms of expressions (9.10) and (9.12) it is clear that viscous dissipation is more likely to be significant when velocities are high and length-scales are large. Thus vigorous flows or flows within geologically sized regions are more likely to display significant viscous dissipative effects. Nield [13] also quotes particle bed nuclear reactors as one other possible area of application where viscous dissipation should not be neglected.

9.3 Free Convective Boundary Layers

9.3.1 Equations of Motion

In this subsection the basic equations (continuity, Darcy, and energy equation) and boundary conditions are written down in the form they apply to the case of free convection over a vertical semi-infinite plate of uniform temperature. Later they are amended according to the physical requirements of forced and mixed convection problems. On applying the boundary-layer approximation ($x \gg y$) and the Boussinesq approximation, the basic equations are (e.g., see Nield and Bejan [17]),

$$\frac{\partial u}{\partial x} + \frac{\partial v}{\partial y} = 0 \tag{9.14}$$

$$\frac{\partial u}{\partial y} = -s_g \frac{g\beta K}{\upsilon}\frac{\partial T}{\partial y} \tag{9.15}$$

$$u\frac{\partial T}{\partial x} + v\frac{\partial T}{\partial y} = \alpha\frac{\partial^2 T}{\partial y^2} + \frac{\upsilon}{Kc_{\mathrm{p}}}u^2 \tag{9.16}$$

and the boundary conditions read

$$v = 0, \quad T = \text{const.} = T_{\mathrm{w}} \quad \text{on } y = 0 \tag{9.17a}$$

$$u \to 0, \quad T \to T_\infty \quad \text{as } y \to \infty \tag{9.17b}$$

Here x and y are the Cartesian coordinates along and normal to the heated surface, respectively, while u and v are the respective velocity components. T is the fluid temperature, K is the permeability of the porous medium, g is the acceleration due to gravity, c_{p} is the specific heat at constant pressure, α, β, and $\upsilon = \mu/\rho$ are the effective thermal diffusivity, thermal expansion coefficient, and kinematic viscosity, respectively. The second term on the right-hand side of Eq. (9.16) is proportional to the volumetric heat generation rate $\Phi = \mu u^2/K$ by viscous dissipation. The origin of the coordinate system is placed on the definite edge of the plate and the positive x-axis is directed along the plate toward its indefinite edge at $x = +\infty$.

For a vertical surface in the presence of viscous dissipation, four physical situations must be distinguished, as depicted schematically in Figure 9.1(a)–(d). The different situations correspond to surfaces that are either upward or downward projecting and are either hot or cold. Mathematically these cases are specified by the signs s_T and s_g where $s_T = \mathrm{sgn}(T_{\mathrm{w}} - T_\infty)$ and where s_g denotes the projection on the positive x-axis of $\mathbf{g}/|\mathbf{g}|$. Thus $s_g = +1$ when the positive x-axis points in the direction of $\mathbf{g}$ (i.e., vertically downwards) and $s_g = -1$ when it points in the direction opposite to $\mathbf{g}$. According to the nomenclature introduced by Goldstein [22] only the "forward" (i.e., the usual) boundary-layer flows will be considered here. These correspond to the cases in which the definite edge of the plate, $x = 0$, represents its leading edge. Their "backward" counterparts, where the definite edge of the plate is a trailing edge, are not considered here. In the case of free convection this means that the backward boundary-layer flows arising in the situations shown in Figure 9.1(b) and (c) will not be discussed in this chapter. Likewise, in the case of forced and mixed convection, it will be assumed that the uniform stream of velocity U_∞ always comes from $x = -\infty$. Thus, in the presence of viscous dissipation, both "aiding" and "opposing" mixed flow regimes can be distinguished. They correspond to Figure 9.1(a) and (d) and 9.1(b) and (c), respectively.

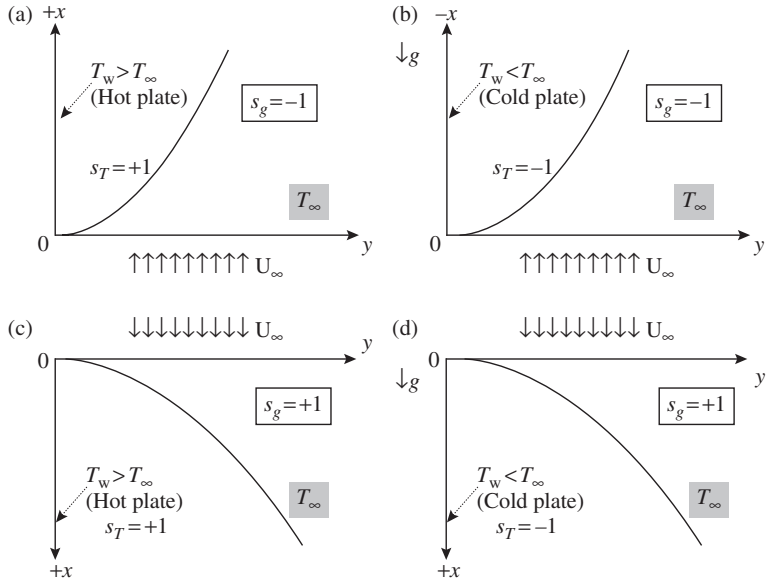

FIGURE 9.1
Representations of the four different mixed convection situations involving either heated or cooled surfaces, and either forward or backward boundary layers. In the absence of viscous dissipation situations (a) and (d) are mathematically identical as are (b) and (c). In the presence of viscous dissipation, the four situations (a), (b), (c), and (d) become physically distinct

9.3.2 Breaking the Upflow/Downflow Equivalence

In the case of free convection, Eqs. (9.15) and (9.17b) yield

$$u = -s_g \frac{g\beta K}{\upsilon}(T - T_\infty) \tag{9.18}$$

After the substitution of,

$$T = T_\infty + s_T |T_w - T_\infty| \cdot \theta \tag{9.19}$$

Equations (9.18), (9.16), and (9.17) become

$$u = -s_g s_T \frac{g\beta K |T_w - T_\infty|}{\upsilon}\theta \tag{9.20}$$

$$u\frac{\partial \theta}{\partial x} + v\frac{\partial \theta}{\partial y} = \alpha \frac{\partial^2 \theta}{\partial y^2} + \frac{s_T \upsilon}{K c_p |T_w - T_\infty|}u^2 \tag{9.21}$$

$$v = 0, \quad \theta = 1 \quad \text{on } y = 0 \tag{9.22a}$$

$$u \to 0, \quad \theta \to 0 \quad \text{as } y \to \infty \tag{9.22b}$$

As mentioned in Section 9.3.1, the forward (or usual) free convection boundary-layer flows, which we are interested in, correspond to the situations shown in Figure 9.1(a) and (d). In both of these cases $s_g s_T = -1$, which, according to Eq. (9.20), implies the same relationship between u and θ. The boundary conditions (9.22), on the other hand, are independent of the signs s_g and s_T. Now, if the viscous dissipation is neglected, Eq. (9.21) also becomes independent of s_T and thus we immediately recover the well-known textbook result concerning the physical equivalence of the free convection flow over an upward projecting hot plate ($s_T = +1$, Figure 9.1[a]) and over its downward projecting cold counterpart ($s_T = -1$, Figure 9.1[d]). If, however, in Eq. (9.21) the viscous dissipation is taken into account, then due to the sign $s_T = \pm 1$ in front of u^2 this physical equivalence gets broken. This means that the free convection flow over the upward projecting hot plate ("upflow," Figure 9.1[a]) and over its downward projecting cold counterpart ("downflow," Figure 9.1[d]) becomes physically distinct. As reported recently [14, 23] one of the dramatic consequences of this broken equivalence is the existence of a strictly parallel free convection flow, the so called ADP, which can only occur over the downward projecting cold plate of Figure 9.1(d) but not over its upward projecting hot counterpart of Figure 9.1(a).

9.3.3 The Asymptotic Dissipation Profile

Introducing the stream function ψ by the usual definition $u = \partial\psi/\partial y$, $v = -\partial\psi/\partial x$ and the dimensionless quantities ξ, Y, and Ψ according to the definitions

$$x = L\xi, \quad y = LR^{-1/2}Y, \quad \psi = \alpha R^{+1/2}\Psi \tag{9.23}$$

where the reference length L and the Darcy–Rayleigh number R are defined as

$$L = \frac{c_{\mathrm{p}}}{g\beta}, \quad R = \frac{g\beta K|T_{\mathrm{w}} - T_\infty|L}{\upsilon\alpha} \tag{9.24}$$

we obtain the quantities θ, u, and v in terms of Ψ as follows

$$\theta = -s_g s_T \frac{\partial\Psi}{\partial Y}, \quad u = \frac{\alpha}{L} R \frac{\partial\Psi}{\partial Y}, \quad v = -\frac{\alpha}{L} R^{1/2} \frac{\partial\Psi}{\partial\xi} \tag{9.25}$$

Here, for the forward boundary-layer flows of Figure 9.1(a) and (d) $s_g s_T = -1$ holds. Thus, we are left with a single unknown function,Ψ, which satisfies

the energy equation

$$\frac{\partial \Psi}{\partial Y}\frac{\partial^2 \Psi}{\partial Y \partial \xi} - \frac{\partial \Psi}{\partial \xi}\frac{\partial^2 \Psi}{\partial Y^2} = \frac{\partial^3 \Psi}{\partial Y^3} - s_g \left(\frac{\partial \Psi}{\partial Y}\right)^2 \tag{9.26}$$

along with the boundary conditions

$$\frac{\partial \Psi}{\partial \xi} = 0 \quad \text{and} \quad \frac{\partial \Psi}{\partial Y} = -s_g s_T = +1 \ \text{ on } \mathrm{Y} = 0 \tag{9.27a}$$

$$\frac{\partial \Psi}{\partial Y} \to 0 \quad \text{as } \mathrm{Y} \to \infty \tag{9.27b}$$

In these dimensionless variables the "broken equivalence" described above becomes manifest again. Indeed, in both the situations shown in Figure 9.1(a) and (d) the boundary conditions (9.27) are the same but due to the presence of s_g in the basic Eq. (9.26) the upward/downward equivalence gets broken.

Our interest in this subsection is in the existence of a strictly parallel-flow solution to the boundary-value problem (9.26), (9.27), that is, on a solution Ψ that depends only on the normal coordinate Y, $\Psi = \Psi(Y)$. Such a solution, if any, satisfies the equation

$$\frac{\mathrm{d}^3 \Psi}{\mathrm{d}Y^3} - s_g \left(\frac{\mathrm{d}\Psi}{\mathrm{d}Y}\right)^2 = 0 \tag{9.28}$$

along with the boundary conditions (9.28). As shown by Magyari and Keller [14] these requirements can only be satisfied for $s_g = +1$ (downflow, Figure 9.1[d]), the corresponding solution being the ADP:

$$\Psi = -\frac{6}{Y + \sqrt{6}}, \quad \theta = \frac{6}{\left(Y + \sqrt{6}\right)^2}, \quad u = \frac{\alpha}{L} R\theta, \quad v = 0 \tag{9.29}$$

Therefore, the ADP is an algebraically decaying parallel-flow solution of the basic Eq. (9.14) to (9.16) of the free convection over a (cold, downward projecting) vertical plate. Its (dimensionless) surface heat flux is given by

$$Q_0 = -\left.\frac{\partial \theta}{\partial Y}\right|_{Y=0} = +\sqrt{\frac{2}{3}} \tag{9.30}$$

and its 1% thickness (i.e., the value Y_δ of Y for which $\theta(Y_\delta) = 0.01$) is $Y_\delta = 9\sqrt{6}$.

The existence of the ADP is quite surprising, since in the absence of viscous dissipation the boundary-value problem (9.14) to (9.17) does not admit

solutions with vanishing transversal component $v = 0$; compared with the parallel component u, the transversal velocity component v is small but always nonvanishing (e.g., see the classical Cheng–Minkowycz solution [21]). The existence of the ADP, however, shows that the (small) buoyancy forces due to heat release by viscous dissipation are able to cancel the (small) transversal component v of the free convection velocity field, thus giving rise to a strictly parallel flow. Such "self-parallelization" of the velocity field in the presence of viscous dissipation can only happen in a free convection flow that descends over a cold plate (downflow), but never in its ascending counterpart over a hot plate (upflow). The reason is that in the latter case, the buoyancy forces due to heat release by viscous dissipation assist the "main" buoyancy forces sustained by the wall temperature gradient, while in the former case of the cold plate, they oppose them.

9.3.4 Flow Development Toward the ADP

The main concern of this section is to discuss the question of whether the ADP solution (9.16) of the boundary-value problem (9.14) to (9.17) represents a physically realizable state of the descending free convection flow or not. The answer, which has been given recently by Rees et al. [23], is that it is realizable. The starting point of the proof given by Rees et al. [23] is the following simple physical reasoning.

In the neighborhood of the leading edge, where the effect of viscous dissipation is negligible, the steady flow has the character of the classical Cheng–Minkowycz boundary-layer solution [21] whose thickness increases with the wall coordinate as $x^{1/2}$. Thus, if the viscous dissipation term in the energy equation is neglected, the boundary-layer thickness grows indefinitely according to the Cheng–Minkowycz similarity solution. This holds both for an ascending free convection flow from a hot plate as well as one descending from a cold plate. But the heat released by viscous dissipation warms up the moving fluid. This in turn accelerates the growth of the ascending boundary layer but decelerates that of the descending one. It is therefore expected that far enough from the leading edge, the thickness of the cold boundary layer will be limited by the warming effect of viscous dissipation to a constant asymptotic value. The limiting state of this boundary-layer flow, which is approached at some distance x_* from the leading edge, should be precisely the ADP which is described by Eq. (9.29).

The numerical experiment of Rees et al. [23] proceeded by first introducing the usual Cheng–Minkowycz similarity variable for boundary-layer flow from a uniform temperature surface in order to describe the beginning stages of the evolution of the flow. Then Eq. (9.26), with $s_g = +1$, were used further downstream. Therefore, the following transformations

$$\eta = \xi^{-1/2} Y, \quad \Psi = \xi^{+1/2} f(\eta, \xi), \quad \theta = \theta(\eta, \xi) \tag{9.31}$$

were substituted into Eq. (9.26) to obtain,

$$f''' + \frac{1}{2}ff'' - \xi f'^2 = \xi\left(f'\frac{\partial f'}{\partial \xi} - f''\frac{\partial f}{\partial \xi}\right), \quad \theta = f' \tag{9.32}$$

where the primes denote differentiation with respect to η. In this form of the basic equations it may be seen explicitly that the viscous dissipation term, $\xi f'^2$, disappears at the origin, where $\xi = 0$.

In numerical simulation, Eq. (9.32) is solved in the range $0 \leq \xi \leq 1$, and Eq. (9.26) in the range $\xi \geq 1$. This means that the developing boundary-layer flow is well approximated near the leading edge, but that the approach to the constant thickness ADP arises naturally within the context of Eq. (9.26). When $\xi \leq 1$, Eq. (9.32) is solved subject to the boundary conditions

$$\eta = 0\text{: } f = 0,\ f' = 1; \quad \eta \to \infty\text{: } f' \to 0 \tag{9.33}$$

but when $\xi > 1$, Eq. (9.26) is solved subject to

$$Y = 0\text{: } \Psi = 0,\ \frac{\partial \Psi}{\partial Y} = 1; \quad Y \to \infty\text{: } \frac{\partial \Psi}{\partial Y} \to 0 \tag{9.34}$$

The respective pairs of equations were solved by a straightforward application of the well-known Keller box method. The solution at the leading edge ($\xi = 0$) is readily seen to satisfy a pair of ordinary differential equations, and the solutions there are the same as those presented by Cheng and Minkowycz [21]. The leading edge profiles were then marched forward in ξ. The accuracy of our numerical scheme is such that the steady value of Q_0 is 0.816454, which has a relative error of 0.00005 on comparison with Eq. (9.30).

Figure 9.2 shows the surface rate of heat transfer in two forms as functions of ξ. More specifically the figure depicts

$$Q_1 = -\xi^{-1/2}\left.\frac{\partial \theta}{\partial \eta}\right|_{\eta=0} \quad \text{for } \xi \leq 1, \quad Q_1 = -\left.\frac{\partial \theta}{\partial Y}\right|_{Y=0} \quad \text{for } \xi \geq 1 \tag{9.35}$$

and

$$Q_2 = -\left.\frac{\partial \theta}{\partial \eta}\right|_{\eta=0} \quad \text{for } \xi \leq 1, \quad Q_2 = -\xi^{+1/2}\left.\frac{\partial \theta}{\partial Y}\right|_{Y=0} \quad \text{for } \xi \geq 1 \tag{9.36}$$

The value Q_1 shows how the surface rate of heat transfer evolves compared with that of the uniform thickness ADP to which the flow tends as $\xi \to \infty$. Near the leading edge the heat transfer is large simply because the boundary layer is thin relative to the ADP. On the other hand, Q_2 represents a rate of heat transfer that is scaled in the same way as for free convection in the absence of viscous dissipation. In this context, the rate of heat transfer increases because the boundary layer becomes relatively thin as ξ increases.

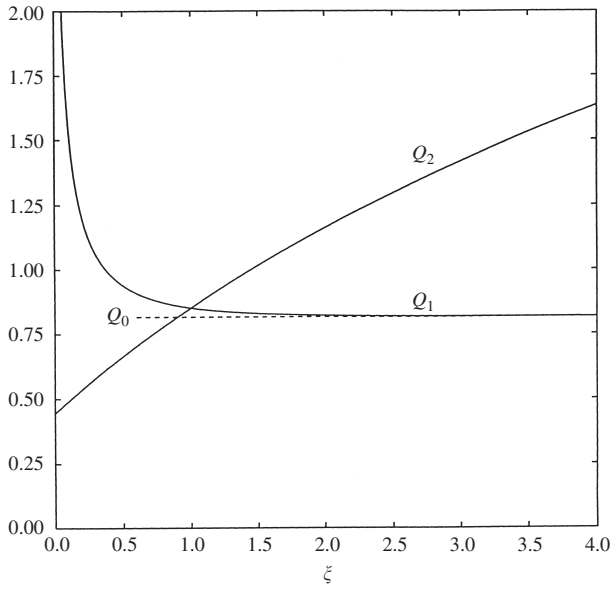

FIGURE 9.2
Variation with ξ of the rate of the heat transfer as represented by Q_1 and Q_2, as defined in Eqs. (9.35) and (9.36), respectively. The Cheng–Minkowycz value of Q_2 is 0.44376 which corresponds to $\xi = 0$. Also shown as a dashed line is the value (9.30) of Q_0 corresponding to the ADP

From the data from which Figure 9.2 was generated, the curve Q_1 is found to be within 1% of the ADP value of $Q_0 = +\sqrt{2/3} = 0.816496$, when $x = 1.79$, and therefore this value may be chosen as being the appropriate value for x_*. In dimensional terms, this is equivalent to

$$x \equiv x_* = 1.79L = 1.79\frac{c_\mathrm{p}}{g\beta} \tag{9.37}$$

which is the distance from the leading edge beyond which the uniform thickness ADP solution applies. The dependence of this "self-parallelization length" of the flow on the parameters β and c_p corresponds to physical expectation. Indeed, the stronger the buoyancy forces, which are proportional to $\rho g\beta\Delta T$, the stronger the self-parallelization effect and accordingly the shorter must be the distance x_*. This explains why both β and g appear in the denominator of Eq. (9.37). Furthermore, the smaller the heat capacity c_p, the larger is the temperature increase due to the heat being released by viscous dissipation, which again shortens the distance x_* at which the growth of the cold boundary-layer ends. This explains the place of c_p in the numerator of Eq. (9.37). It should be underlined here that in usual applications the order of magnitude of x_* amounts to several kilometers so that self-parallelization of free convection flows due to dissipative effects is likely to occur only in geologically sized applications.

9.3.5 Other Free Convective Flows

We now discuss briefly other works on free convection boundary-layer flows where viscous dissipation has been included in the thermal energy equation.

A rather early paper by Nakayama and Pop [4] discusses free convection induced by a heated surface of arbitrary shape, of which a flat plate and a horizontal cylinder are but two special cases. Their analysis proceeds by expanding the governing nonsimilar boundary-layer equations as a series solution in εx, where ε is the Gebhart number, and solving the resulting systems of ordinary differential equations using the Karman–Pohlhausen integral technique. It was found that the presence of viscous dissipation reduces the heat flux from the heated surface, in general. They also obtained similarity solutions for certain special variations in the surface temperature when the heated surface is vertical.

Murthy and Singh [24] and Murthy [25] also used a small-ε expansion in their study of Darcy–Forchheimer convection from a vertical surface. In addition these authors used a velocity-dependent thermal diffusivity. Once more it was found that the surface rate of heat transfer decreases as the Gebhart number increases from zero.

The vertical plate was also considered by Takhar et al. [26] using the Darcy–Brinkman model for the momentum equations. However, the formula for viscous dissipation which was used by those authors corresponds to that for a clear fluid, rather than one of the forms given by Eqs. (9.7) or (9.8). Unfortunately, a similar use of the clear fluid model may be found in the papers by Kumari and Nath [27], Yih [28], El-Amin [29], and Israel-Cookey et al. [30], who study boundary-layer flows in the presence of a magnetic field, and in the mixed convection paper by Kumari et al. [31].

Sections 9.3.3 and 9.3.4 reported the situation for Darcy flow over a downward projecting cold plate. When the plate is upward and hot (i.e., it corresponds to Figure 9.1[a]), then the flow may be computed by solving Eq. (9.32) but with the viscous dissipation term having the opposite sign. Preliminary studies by the authors show that the boundary layer becomes exponentially thin as ξ increases, and the temperature becomes exponentially large due to the positive feedback between buoyancy and viscous dissipation; this will be reported in due course.

9.4 Forced Convection with Examples

9.4.1 Boundary-Layer Analysis

In this section, we consider a uniform forced convection flow of an incompressible fluid with imposed velocity $\mathbf{v} = (u, 0, 0)$, where $u = \text{const.} \equiv U_\infty$ within a porous medium extending to $x \geq 0, y \geq 0$, as shown in Figure 9.1(a). Thus fluid enters the porous domain at $x = 0$. The only governing

equation is the energy equation (9.16) which in this case reduces to

$$U_\infty \frac{\partial T}{\partial x} = \alpha \frac{\partial^2 T}{\partial y^2} + \frac{\upsilon}{Kc_\mathrm{p}} U_\infty^2 \tag{9.38}$$

where it has been assumed that streamwise diffusion is negligible (i.e., that the boundary-layer approximation applies). The temperature of the porous boundary at $x = 0$ (termed the entrance boundary) coincides with the constant temperature T_∞ of the entering fluid,

$$T(0, y \geq 0) = T_\infty \tag{9.39}$$

and the temperature of the impermeable plane surface $y = 0$ adjacent to the porous medium (termed the adjacent surface) is now a given function of the coordinate x,

$$T(x \leq 0, 0) = T_\infty, \quad T(x > 0, 0) = T_\mathrm{w}(x) \tag{9.40}$$

The general physical requirement that no heat "disappears" at infinity reads:

$$\frac{\partial T}{\partial y}(x \geq 0, \infty) = 0 \tag{9.41}$$

Now, it is immediately seen that in such a forced convection problem the "usual" far-field condition, namely, $T(x > 0, \infty) = \text{const.} = T_\infty$ is inconsistent with the energy equation (9.38); since it implies that $U_\infty = 0$, which is contrary to the assumption. Instead, Eqs. (9.38) and (9.41) imply in this case

AQ: Please check the insertion of zero in eq. (9.42). Is it ok?

$$\frac{\partial T}{\partial x}(x \geq 0, \infty) = \frac{\upsilon U_\infty}{Kc_\mathrm{p}} \tag{9.42}$$

which further yields

$$T(x \geq 0, \infty) = T_\infty + \frac{\upsilon U_\infty}{Kc_\mathrm{p}} x \tag{9.43}$$

Hence the only far-field condition which is consistent with the energy equation is given by Eq. (9.43). It specifies an asymptotic temperature that is not a constant, but a linear function of the wall coordinate x. This condition applies both for the forced and the mixed convection problems in extended porous media when the effect of viscous dissipation is taken into account [6].

We may conclude, then, that it is not possible to set a far-field temperature profile when considering mixed or forced convection in the presence of viscous dissipation. This result is in full agreement with physical expectation. Indeed, in contrast to free convection where the flow velocity goes to

zero as $y \to \infty$, in the forced and mixed convection boundary-layer flows where $U_\infty = \text{const.} \neq 0$, the mechanical power needed to extrude the fluid through the pores continues to generate frictional heat in the asymptotic region $y \to \infty$. Practically, the correct numerical solutions may be obtained by applying either Eq. (9.41) or Eq. (9.43) as $y \to \infty$. It may also be seen that Eq. (9.38) is mathematically equivalent to Fourier's equation for heat conduction in a semi-infinite homogeneous solid with uniform volumetric heat generation (where x is regarded as the time variable). Thus, after an infinitely long time (i.e., as $x \to \infty$), the whole solid must become infinitely hot in accordance with Eq. (9.43).

For more transparency, it is convenient to introduce a reference length L, a reference temperature $T_{\text{ref}} > T_\infty$, and define the Eckert, Prandtl, Darcy, and Péclet numbers in terms of these quantities as follows:

$$Ec = \frac{U_\infty^2}{c_{\text{p}}(T_{\text{ref}} - T_\infty)}, \quad Pr = \frac{\mu}{\rho\alpha}, \quad Da = \frac{K}{L^2}, \quad Pe = \frac{U_\infty L}{\alpha} \tag{9.44}$$

Thus, the asymptotic condition (9.43) becomes

$$T(x \geq 0, \infty) = T_\infty + (T_{\text{ref}} - T_\infty)\tilde{E}c\frac{x}{L} \tag{9.45}$$

where $\tilde{E}c$ is a "modified Eckert number" defined as

$$\tilde{E}c = \frac{Ec \cdot Pr}{Da \cdot Pe} = \frac{\mu U_\infty L}{K\rho c_{\text{p}}(T_{\text{ref}} - T_\infty)} \tag{9.46}$$

Alternatively, it is convenient to use the "local" counterparts of these quantities, which can be obtained by substituting L in Da and Pe simply by x. Thus the "local modified Eckert number" $\tilde{E}c_x$, the counterpart of $\tilde{E}c$, is

$$\tilde{E}c_x = \frac{Ec \cdot Pr}{Da_x \cdot Pe_x} = \tilde{E}c\frac{x}{L} \tag{9.47}$$

Now, the analytical solution of Eq. (9.38) for some realistic temperature distributions $T_{\text{w}} = T_{\text{w}}(x)$ of the adjacent surface $y = 0$ will be given. To this end, we first make the change of variables

$$T(x, y) = T_\infty + (T_{\text{ref}} - T_\infty)\frac{U_\infty \cdot \tilde{E}c}{L}\tau + \theta(\tau, y), \quad \tau = \frac{x}{U_\infty} \tag{9.48}$$

and Eq. (9.38) becomes:

$$\frac{\partial\theta}{\partial\tau} = \alpha\frac{\partial^2\theta}{\partial y^2} \tag{9.49}$$

on taking into account that

$$T(x,y) = T_\infty + (T_{\text{ref}} - T_\infty)\tilde{E}c\frac{x}{L} \tag{9.50}$$

represents the exact solution of Eq. (9.38) corresponding to $\alpha = 0$. Equation (9.48) implies that the quantity $\theta\left(\tau, y\right)$ describes precisely the contribution of heat diffusion in the y-direction to the temperature field $T(x,y)$ in addition to the effect of viscous dissipation and convection. Accordingly, Eq. (9.49) coincides formally with Fourier's equation of heat conduction in a homogeneous solid of thermal diffusivity α, where the role of time variable is played by $\tau = x/U_\infty$ and where now the above-mentioned uniform heat generation has been removed by transformation (9.48). In this way, our forced convection heat transfer problem reduces to one of a transient heat conduction problem in a semi-infinite solid occupying the region $y > 0$ and subject to the initial condition,

$$\theta(0, y \geq 0) = 0 \tag{9.51}$$

As a consequence of Eqs. (9.48) and (9.40) the temperature at the boundary at $y = 0$ is given by

$$\theta(\tau > 0, 0) = T_{\text{w}}(x) - T_\infty - (T_{\text{ref}} - T_\infty)\frac{U_\infty \cdot \tilde{E}c}{L}\tau \equiv \theta_{\text{w}}(\tau) \tag{9.52}$$

The solution of the heat conduction problem (9.49), (9.51), (9.52) is well known (e.g., see Carslaw and Jaeger [32], section 9.2.5) and reads:

$$\theta(\tau, y) = \frac{2}{\sqrt{\pi}}\int_\eta^\infty \theta_{\text{w}}\left(\tau - \frac{y^2}{4\alpha\xi^2}\right)\mathrm{e}^{-\xi^2}\mathrm{d}\xi \tag{9.53}$$

where

$$\eta = \sqrt{Pe}\frac{y}{2\sqrt{Lx}} = \sqrt{Pe_x}\frac{y}{2x} \tag{9.54}$$

In this way, the temperature profiles $\theta = \theta(\tau, y)$ of the solid at different "instants" $\tau = x/U_\infty$ determine the temperature profiles of the uniformly moving fluid in our porous body at different distances x from the entrance boundary $x = 0$. This analogy allows us to transcribe easily the exact solution of several well-known heat conduction problems listed, for example, in Carslaw and Jaeger [32] for the case of the present forced convection problem.

A part of the integrations in (9.53) with $\theta_{\text{w}}(\tau)$ given by Eq. (9.52) can be performed without the need to specify the surface temperature distribution

$T_w(x)$ explicitly. Thus we obtain the following general expression for the temperature field:

$$\frac{T(x,y)-T_{ref}}{T_{ref}-T_\infty} = \tilde{E}c_x(1-4i^2\mathrm{erf}\,c\eta) - \mathrm{erf}\,\eta - \frac{1}{T_{ref}-T_\infty}\left(T_{ref}\mathrm{erf}\,c\eta - \frac{2}{\sqrt{\pi}}\int_\eta^\infty T_w\left(x-\frac{x\eta^2}{\xi^2}\right)e^{-\xi^2}d\xi\right) \tag{9.55}$$

Here, $\mathrm{erf}\,\eta$ and $\mathrm{erf}\,c\eta = 1 - \mathrm{erf}\,\eta$ denote the error and complementary error functions respectively, where $i^n\mathrm{erf}\,c\eta$ stands for the nth repeated integrals of the error function (see Carslaw and Jaeger [32], appendix II).

The remainder of this section is devoted to two explicit examples. The quantities of physical interest will be the temperature field $T(x,y)$ and the wall heat flux

$$q_w(x) = -k\frac{\partial T}{\partial y}(x,0) = -k\frac{\partial \theta}{\partial y}(\tau,0) \tag{9.56}$$

corresponding to a prescribed temperature distribution $T_w(x)$ of the adjacent plane surface $y = 0$. The local Nusselt number related to (9.33) will be defined in this chapter as follows

$$Nu_x = \frac{q_w(x)\cdot x}{k(T_{ref}-T_\infty)} \tag{9.57}$$

Note that in the denominator the same temperature difference has been included as in the definition (9.44) of the Eckert number.

Example 1. The most simple mathematical example is obtained for $\theta_w(\tau) \equiv 0$ when the integral (9.53) is vanishing and thus $\theta(\tau,y) \equiv 0$. According to Eq. (9.52), this case corresponds to the temperature distribution

$$T_w(x) = T_\infty + (T_{ref}-T_\infty)\tilde{E}c_x \tag{9.58}$$

of the adjacent surface, which as $\theta(\tau,y) \equiv 0$, becomes identical with the solution (9.48) for the problem, $T_w(x) = T(x,y)$. This coincides further with the temperature field (9.50) found in the purely convective case ($\alpha = 0$). Accordingly, the linear heating law (9.58) of the adjacent surface has the consequence that (a) the wall heat flow is identically vanishing, $q_w(x) \equiv 0$, and (b) nowhere in the bulk of the fluid does heat diffusion occur.

AQ: Please check if the edits have retained the intended sense of the sentence 'This case...'

Example 2. As a second simple example, we consider the case $\theta_w(x) = \text{const.} \equiv T_{ref} - T_\infty \equiv T_0 - T_\infty > 0$, which corresponds to the wall temperature distribution

$$T_w(x) = T_0 + (T_0-T_\infty)\tilde{E}c_x \tag{9.59}$$

In this case, the integral (9.53) yields $\theta(\tau, y) = (T_0 - T_\infty)\text{erf}\, c\eta$ and the solution (9.48) becomes

$$T(x, y) = T_0 + (T_0 - T_\infty)(\tilde{E}c_x - \text{erf}\, \eta) \tag{9.60}$$

When $y \to \infty$, we easily recover the far-field relationship (9.45). For $\mu = 0$, that is, in the absence of viscous dissipation, Eq. (9.59) reduces to $T_\text{w}(x) = T_0$ and in Eq. (9.60) we immediately recover Bejan's classical result [3,17]:

$$T(x, y) = T_0 - (T_0 - T_\infty)\text{erf}\, \eta \tag{9.61}$$

The wall heat flux and the local Nusselt number corresponding to the temperature field (9.60) are given by

$$q_\text{w}(x) = \frac{k(T_0 - T_\infty)}{x}\sqrt{\frac{Pe_x}{\pi}} \tag{9.62}$$

$$Nu_x = \sqrt{\frac{Pe_x}{\pi}} \tag{9.63}$$

Note that Bejan's solution (9.61) for the forced convection flow over the adjacent plane surface of constant temperature T_0 without viscous dissipation also leads to the same expressions (9.62) and (9.63) that have been obtained from the present result (9.60). In the present case, however the surface temperature is not a constant but a linear function of x, being given by Eq. (9.59). Hence, compared to the constant surface temperature without viscous dissipation, the linear increase of $T_\text{w}(x)$ according to Eq. (9.59) represents the surface temperature distribution that exactly removes the effect of the viscous dissipation on the surface heat flow.

Finally, it is worth underlining again that for a consistent description of the forced and mixed convection problems in fluid saturated porous media in the presence of viscous dissipation the usual far-field condition must be substituted by

$$T(x \geq 0, \infty) = T_\infty + (T_\text{ref} - T_\infty)\tilde{E}c\frac{x}{L} = T_\infty + (T_\text{ref} - T_\infty)\tilde{E}c_x \tag{9.64}$$

As a consequence, several recent publications concerning the mixed convection problems in the presence of viscous dissipation must basically be revised (for more details see the next section).

9.4.2 Channel Flows

Till date only two papers exist that deal with forced convective flows in channels in the presence of viscous dissipation. The papers by Nield et al. [33]

and Kuznetsov et al. [34] are two in a series of papers by the same authors that consider porous medium versions of the classical Graetz problem. In this problem fully developed flow exists in a uniform channel that points in the x-direction where the boundary temperature is set at T_0 when $x < 0$, and where the temperature of one or both surfaces (or the surface in the case of a circular pipe) is raised to T_1 when $x > 0$. The strength of the flow is measured in terms of the Péclet number, *Pe*, and the classical Graetz problem analyses the thin thermal boundary layer that exists downstream of $x - 0$ when the Péclet number is large. The strength of the viscous dissipation effect is measured by the size of the Brinkman number, *Br*.

In the above-quoted papers these authors study cases where *Pe* is not large using a series expansion method. Nield et al. [33] consider a plane channel while Kuznetsov et al. [34] apply the same methodology to a circular pipe flow. In both cases, the authors found that variations in the value of *Br* affect the surface rates of heat transfer very considerably. The authors also investigated the differences in the results obtained by each of the three models of viscous dissipation given by Eqs. (9.3), (9.7), and (9.8). It was found that the corresponding far downstream values of the Nusselt number differ appreciably only when the Darcy number is of magnitude unity or higher, that is, in cases where the porous medium is very highly porous.

9.5 Mixed Convection

9.5.1 The Darcy–Forchheimer Flow

In this section and in Sections 9.5.2 and 9.5.3, we consider the mixed convection case of a Darcy–Forchheimer steady-boundary-layer flow over an isothermal vertical flat plate in the physical situations depicted in Figure 9.1(a)–(d). Following Murthy [8] and the notation used in Eqs. (9.1) to (9.3), we write the mass, momentum, and energy balance equations (subject to both the boundary layer and Boussinesq approximations) in the form

$$\frac{\partial u}{\partial x} + \frac{\partial v}{\partial y} = 0 \tag{9.65}$$

$$\frac{\partial}{\partial y}\left(u + \frac{C\sqrt{K}}{\upsilon}u^2\right) = -s_g \frac{Kg\beta}{\upsilon}\frac{\partial}{\partial y}(T - T_\infty) \tag{9.66}$$

$$u\frac{\partial T}{\partial x} + v\frac{\partial T}{\partial y} = \alpha\frac{\partial^2 T}{\partial y^2} + \frac{\upsilon}{Kc_{\mathrm{p}}}u \cdot \left(u + \frac{C\sqrt{K}}{\upsilon}u^2\right) \tag{9.67}$$

and the corresponding boundary conditions in the form [8]

$$y = 0\text{: } v = 0, \quad T = \text{const.} \equiv T_{\mathrm{w}} \tag{9.68a,b}$$

$$y \to \infty: u \to U_\infty, \quad T \to T_\infty \tag{9.69a,b}$$

where C denotes the Forchheimer form drag coefficient.

Now, it is immediately seen that the thermal far-field condition (9.69b) is not suitable since, as discussed in Section 9.4, it is inconsistent with the energy equation. Indeed, having in mind Eq. (9.41), the energy equation (9.67) requires

$$\lim_{y\to\infty} \frac{\partial T}{\partial x} = \frac{\upsilon U_\infty}{K c_{\mathrm{p}}}(1 + Re) \tag{9.70}$$

where

$$Re = \frac{C U_\infty \sqrt{K}}{\upsilon} \tag{9.71}$$

denotes the modified Reynolds number. Thus, integrating Eq. (9.70) once and taking into account condition (9.39) at the entrance boundary we obtain

$$T(x, \infty) = T_\infty + \frac{\upsilon U_\infty}{K c_{\mathrm{p}}}(1 + Re)x \tag{9.72}$$

Therefore, a consistent description of the present mixed convection problem requires us to replace the (unsuitable) boundary condition (9.69b) by the condition (9.72), that is

$$y \to \infty: u \to U_\infty, T \to T_\infty + \frac{\upsilon U_\infty}{K c_{\mathrm{p}}}(1 + Re)x \tag{9.73a,b}$$

With the aid of the pseudo-similarity transformation [8]

$$\begin{aligned} \eta &= \frac{y}{x}\sqrt{Pe_x} \\ \psi &= \alpha\sqrt{Pe_x} \cdot f(x, \eta) \\ T &= T_\infty + s_T \cdot |T_{\mathrm{w}} - T_\infty|\theta(x, \eta), \quad s_T = \mathrm{sgn}(T_{\mathrm{w}} - T_\infty) \end{aligned} \tag{9.74}$$

and the usual definition of the stream function, $u = \partial\psi/\partial y$ and $v = -\partial\psi/\partial x$, we transform Eqs. (9.66) and (9.67) in

$$f'' + 2Re \cdot f' \cdot f'' = -s_g s_T \frac{R_x}{Pe_x}\theta' \tag{9.75}$$

$$\theta'' + \frac{1}{2}f\theta' + s_T \frac{Pe_x}{R_x}\varepsilon f'^2(1 + Re \cdot f') = \varepsilon\left(f'\frac{\partial\theta}{\partial\varepsilon} - \theta'\frac{\partial f}{\partial\varepsilon}\right) \tag{9.76}$$

and the boundary conditions (9.68) and (9.73) in

$$\eta = 0: f(x,0) + 2x\frac{\partial f}{\partial x}(x,0) = 0, \quad \theta(x,0) = 1 \tag{9.77a,b}$$

$$\eta \to \infty: f'(x,\infty) = 1, \quad \theta(x,\infty) = s_T \frac{Pe_x}{R_x}(1+Re)\varepsilon \tag{9.78a,b}$$

where the prime denotes derivatives with respect to the similarity variable η. The local Darcy–Rayleigh number R_x that occurs in the above equations is obtained by substituting in Eq. (9.24) the reference length L by the wall coordinate x while ε stands for the local Gebhart number

$$Ge_x = \frac{\beta g x}{c_p} \equiv \varepsilon \tag{9.79}$$

Thus, the ratio Pe_x/R_x is in fact independent of x. Now, integrating Eq. (9.75) once and determining the (ε-dependent) integration constant by taking into account the boundary condition (9.78) we obtain

$$f' \cdot (1 + Re \cdot f') = (1+Re)(1+s_g\varepsilon) - s_g s_T \frac{R_x}{Pe_x}\theta \tag{9.80}$$

which when substituted in Eq. (9.76) results in

$$\theta'' + \frac{1}{2}f\theta' - \varepsilon f'\left[s_g\theta - s_T\frac{Pe_x}{R_x}(1+Re)(1+s_g\varepsilon)\right] = \varepsilon\left(f'\frac{\partial\theta}{\partial\varepsilon} - \theta'\frac{\partial f}{\partial\varepsilon}\right) \tag{9.81}$$

We note that the boundary condition (9.77a) can be reduced to $f(x,0) = 0$ by assuming that $f(0,0) = 0$. Indeed, a formal integration of Eq. (9.77a) yields $f(x,0) = \text{const.} \cdot x^{-1/2}$, which results precisely in $f(x,0) = 0$ if one assumes $f(0,0) = 0$. Hence, for a consistent solution of the present mixed convection problem we must consider Eq. (9.81) and Eq. (9.75), or the first integral of Eq. (9.75) given by Eq. (9.80), along with the boundary conditions

$$\eta = 0: f(x,0) = 0, \quad \theta(x,0) = 1 \tag{9.82a,b}$$

$$\eta \to \infty: f'(x,\infty) = 1, \quad \theta(x,\infty) = s_T \frac{Pe_x}{R_x}(1+Re)\varepsilon \tag{9.83a,b}$$

In this way, the main difference compared with the work of earlier authors are (a) of the boundary condition (9.83b), instead of $\theta(x,\infty) = 0$

and (b) of the second term occurring in the square bracket of Eq. (9.81).

9.5.2 Perturbation Approach for Small Gebhart Number

For small values of the local Gebhart number $\varepsilon = g\beta x/c_{\mathrm{p}}$, the above boundary-value problem can be solved by a perturbation approach based on the series expansions [8].

$$\begin{aligned} f(x,\eta) &= \sum_{m=0}^{\infty}(-1)^m \varepsilon^m f_m(\eta) \\ \theta(x,\eta) &= \sum_{m=0}^{\infty}(-1)^m \varepsilon^m t_m(\eta) \end{aligned} \tag{9.84}$$

with which we proceed here up to order ε^2, that is,

$$\begin{aligned} f(x,\eta) &= f_0(\eta) - \varepsilon f_1(\eta) + \varepsilon^2 f_2(\eta) \\ \theta(x,\eta) &= t_0(\eta) - \varepsilon t_1(\eta) + \varepsilon^2 t_2(\eta) \end{aligned} \tag{9.85}$$

Thus, after some algebra we obtain, to orders 0, 1, and 2 in ε, the following systems of ordinary differential equations and boundary conditions.

To order ε^0:

$$\begin{gathered} f_0' + Re\, f_0'^2 + s_g s_T \frac{R_x}{Pe_x} t_0 = 1 + Re \\ t_0'' + \frac{1}{2} f_0 t_0' = 0 \\ f_0(0) = 0, \quad f_0'(\infty) = 1, \quad t_0(0) = 1, \quad t_0(\infty) = 0 \end{gathered} \tag{9.86}$$

To order ε^1:

$$\begin{gathered} f_1' + 2Re\, f_0' f_1' + s_g s_T \frac{R_x}{Pe_x} t_1 = -s_g(1 + Re) \\ t_1'' + \frac{1}{2}(f_0 t_1' + t_0' f_1) + s_g f_0' t_0 + f_1 t_0' - f_0' t_1 = s_T \frac{Pe_x}{R_x}(1 + Re) f_0' \\ f_1(0) = 0, \quad f_1'(\infty) = 0, \quad t_1(0) = 0, \quad t_1(\infty) = -s_T \frac{Pe_x}{R_x}(1 + Re) \end{gathered} \tag{9.87}$$

To order ε^2:

$$f_2' + Re\left(2f_0'f_2' + f_1'^2\right) + s_g s_T \frac{R_x}{Pe_x} t_2 = 0$$

$$t_2'' + \frac{1}{2}\left(f_0 t_2' + f_1 t_1' + t_0' f_2\right) + s_g\left(f_0' t_1 + f_1' t_0\right) + f_1 t_1' - f_1' t_1 + 2\left(t_0' f_2 - f_0' t_2\right)$$
$$= s_T \frac{Pe_x}{R_x}(1 + Re)\left(f_1' - s_g f_0'\right)$$
$$f_2(0) = 0, \quad f_2'(\infty) = 0, \quad t_2(0) = 0, \quad t_2(\infty) = 0 \tag{9.88}$$

On comparing these system of equations with the corresponding equations of earlier authors, one sees that the essential difference between the present analysis and others comes from the nonvanishing right-hand sides of the equations for t in (9.87) and (9.88) and in the asymptotic condition in (9.87) for $t_1(\infty)$.

9.5.3 The Aiding Up- and Downflows

In order to be more specific we restrict the discussion to the Darcy mixed convection flows ($Re = 0$) for the two "aiding" cases corresponding to the physical situations shown in Figure 9.1(a) (upward projecting hot plate in assisting stream) and 9.1(d) (downward projecting cold plate in assisting stream), respectively. In both of these cases we have $s_T \cdot s_g = -1$. In addition, we chose $R_x/Pe_x = 1$.

For these parameter values the following simple relationships hold:

$$f'(x,\eta) = 1 + s_g\varepsilon + \theta(x,\eta), \quad f'(x,0) = 2 + s_g\varepsilon \tag{9.89a}$$
$$f_0'(\eta) = 1 + t_0(\eta), \quad f_0'(0) = 2 \tag{9.89b}$$
$$f_1'(\eta) = -s_g + t_1(\eta), \quad f_1'(0) = -s_g \tag{9.89c}$$
$$f_2'(\eta) = t_2(\eta), \quad f_2'(0) = 0 \tag{9.89d}$$
$$f''(x,\eta) = \theta'(x,\eta) \tag{9.90}$$

Equation (9.89a) represents a modified form of the Reynolds analogy known from the viscous flow of clear fluids.

We first solved the boundary-value problems (9.86) to (9.88) corresponding to the case of the hot plate (Figure 9.1[a], $s_T = +1, s_g = -1$) with the aid of the familiar shooting method, obtaining for the missing "initial values" the numerical results,

$$\begin{aligned} t_0'(0) &= -0.7205853 \\ t_1'(0) &= -2.41893785 \quad \text{(hot plate, } s_T = +1, s_g = -1\text{)} \\ t_2'(0) &= -0.794596877 \end{aligned} \tag{9.91}$$

It is worth mentioning that the numerical calculations becomes more and more sensitive with increasing order of the approximation.

Owing to some simple symmetry considerations, the case of the cold plate (Figure 9.1[d], $s_T = -1$, $s_g = +1$) does not require new numerical effort. Indeed, all our basic equations and boundary conditions (9.80) to (9.83) are invariant under the sign-change transformation $(s_T, s_g, \varepsilon) \to (-s_T, -s_g, -\varepsilon)$. As a consequence, all the perturbation equations and boundary conditions (9.86) to (9.88) are invariant under the transformation

$$(s_T, s_g, f_1, t_1) \to (-s_T, -s_g, -f_1, -t_1) \tag{9.92}$$

This means that in the case of the cold plate (Figure 9.1[d], $s_T = -1, s_g = +1$) the missing "initial values" can be obtained from Eqs. (9.91) by only changing the sign of $t_1'(0)$:

$$\begin{array}{l} t_0'(0) = -0.7205853 \\ t_1'(0) = +2.41893785 \quad \text{(cold plate, } s_T = -1, s_g = +1\text{)} \\ t_2'(0) = -0.794596877 \end{array} \tag{9.93}$$

The local Nusselt number, defined according to Eq. (9.57) with $T_{\text{ref}} \equiv T_{\text{w}}$, can thus be calculated to order ε^2 as

$$\frac{Nu_x}{\sqrt{Pe_x}} = -\theta'(x,0) = s_T \cdot \left[-t_0'(0) + \varepsilon t_1'(0) - \varepsilon^2 t_2'(0)\right] \tag{9.94}$$

In Figure 9.3, $Nu_x/\sqrt{Pe_x}$ is plotted for the two mixed convection flows as a function Gebhart number ε. The difference Δ of the absolute values of the amount of heat transferred in these two cases as given by

$$\Delta = \left|\frac{Nu_x}{\sqrt{Pe_x}}\right| \text{(cold plate)} - \left|\frac{Nu_x}{\sqrt{Pe_x}}\right| \text{(hot plate)} \tag{9.95}$$

is also shown in Figure 9.3.

As expected, in the case of the cold plate the heat transfer coefficient is negative, that is, heat is always transferred from the fluid to the wall. This amount of heat increases with increasing value of the local Gebhart number ε (from 0.72058 if the viscous dissipation is neglected, $\varepsilon = 0$, to 2.128703 for $\varepsilon = 0.5$). In the case of the hot plate, the heat transfer coefficient is positive (i.e., heat is transferred from the wall to the fluid) as long as the effect of viscous dissipation is weak enough which means $\varepsilon < 0.3346898$. When ε exceeds this critical value $\varepsilon_{\text{c}} = 0.3346898$ the heat released by viscous dissipation overcomes the effect of the hot wall and the wall heat flux becomes reversed. For $\varepsilon = \varepsilon_{\text{c}}$ the wall becomes adiabatic. As the thin curve of Figure 9.3 shows, for the same value of ε, the amount of heat transferred to the cold plate always exceeds the amount of heat transferred from, as well as, to the hot plate.

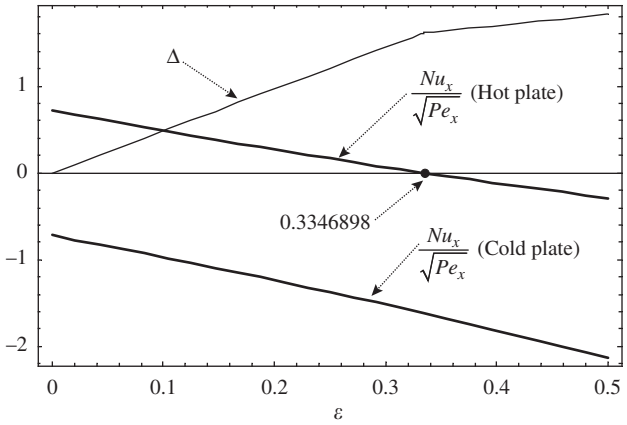

FIGURE 9.3
Heat-transfer coefficients (9.94) for two types of aided mixed convection flows along an upward projecting hot plate (Figure 9.1[a]) and a downward projecting cold plate (Figure 9.1[d]). The thin curve represents the difference Δ between the absolute values of the amount of heat transferred in these two cases, as given by Eq. (9.95)

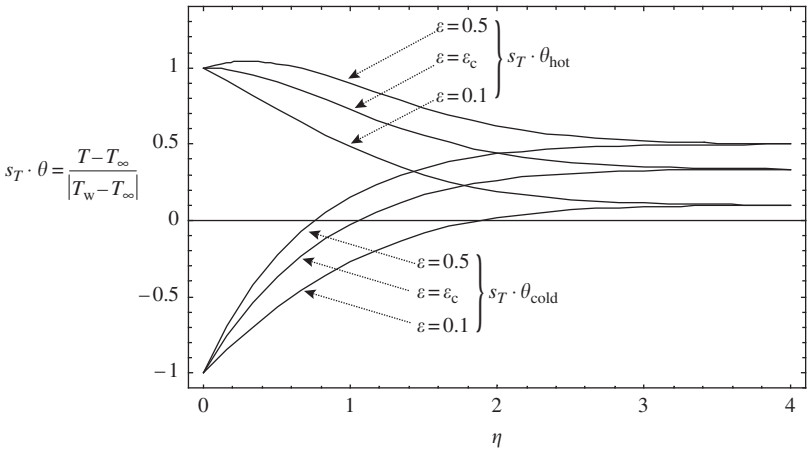

FIGURE 9.4
Dimensionless temperature profiles $s_T \cdot \theta_{hot} = +\theta_{hot}$ and $s_T \cdot \theta_{cold} = -\theta_{cold}$ corresponding to the two cases of aided Darcy mixed convection flow (Figures 9.1[a] and [d], respectively). The critical value $\varepsilon_c = 0.3346898$ corresponds to the adiabatic case of the hot plate

In Figure 9.4 the dimensionless temperature profiles $s_T \cdot \theta = (T - T_\infty)/|T_w - T_\infty|$ are shown for $s_T = +1$ and -1 and a couple of values of ε. The change from the direct to reversed wall heat flux at the critical Gebhart number $\varepsilon_c = 0.3346898$ in the case of the hot plate is immediately seen in this figure. It is also clearly seen that, according to the boundary condition (9.83b), both the dimensionless temperature profiles $s_T \cdot \theta_{hot} = +\theta_{hot}$ and $s_T \cdot \theta_{cold} = -\theta_{cold}$ approach the same asymptotic value $s_T \cdot \theta(x, \infty) = \varepsilon$ as $\eta \to \infty$. This is in

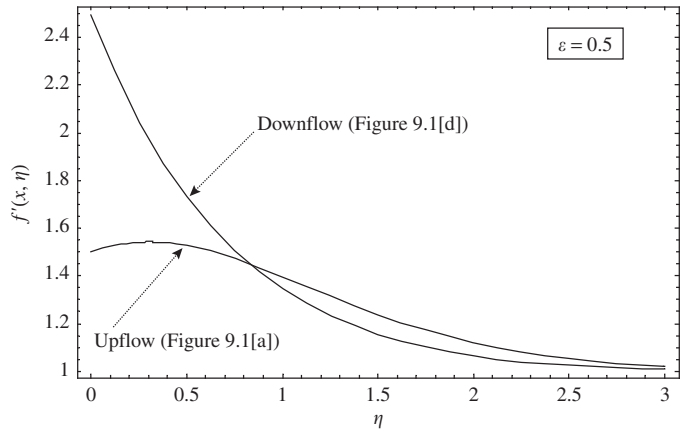

FIGURE 9.5
Dimensionless downstream velocity profiles corresponding to two cases of aided Darcy mixed convection flow (Figures 9.1[a] and [d], respectively)

whole agreement with the special case $\{Re = 0, R_x/Pe_x = 1\}$ of the boundary condition (9.73b).

Finally in Figure 9.5 the dimensionless downstream velocity profiles $f'(x, \eta)$ are shown for $\varepsilon = 0.5$. Figure 9.4 and Figure 9.5 are related to each other by Eq. (9.89a), which may be checked easily.

9.5.4 Channel Flows

Ingham et al. [5] and Al-Hadhrami et al. [35] have both considered mixed convection in a vertical porous channel in the presence of viscous dissipation. In both cases the bounding surfaces have a temperature that is a linear decreasing function of height, that is, the channel is unstably stratified, and there is a fixed local temperature difference across the channel. Ingham et al. [5] used the Darcy flow model and determined the basic flow and temperature fields. In the absence of viscous dissipation the governing equations yield singular solutions when the Rayleigh number, Ra, is such that $Ra^{1/2}$ is an odd multiple of π. When viscous dissipation is included, then the singularity disappears, and is replaced by a pair of solutions, one of which corresponds to the limit as Ra tends upward toward a critical value, and the other as Ra tends downward toward the same value. Al-Hadhrami et al. [35] extended the analysis to cases where the Darcy–Brinkman model apply. The same qualitative results appear here too, but they also show that multiple solutions arise in general.

9.6 Stability Considerations

The study of viscous dissipation in porous media cannot yet be considered to be a mature realm of science for a variety of reasons, not the least of which

is the uncertainty as to how it should be modeled when the Brinkman terms are significant in the momentum equations. It might therefore seem a little premature to consider whether or not the flows discussed herein are realizable in practice, should they suffer small perturbations. Given that there appears to be general agreement in the published literature over the form that the viscous dissipation terms take when the flow obeys Darcy's law, it is important that some studies are undertaken to assess the stability characteristics of some flows. At present only two such studies have been undertaken. Rees et al. [35] analyzed the linear stability of the ADP from an inclined surface, while Rees et al. [15] reworked the standard weakly nonlinear analysis for the case of Darcy–Benard convection given in Rees [36]. This section briefly summarizes the chief features of these analyses because the details are beyond the space available.

When a cold downward-projected surface is rotated so that it is inclined away from the vertical, and in such a way that the normal vector to the cold surface has a downward component, then the ADP analysis described earlier still applies but the parallel-flow boundary layer is thicker because buoyancy is less effective. The expression for θ is given by Eq. (9.29), but with Y replaced by $Y\cos\alpha$, where α is the inclination of the surface from the vertical. In such situations it is possible to introduce disturbances of the form of streamwise vortices. A straightforward linearized stability theory yields a curve relating the Rayleigh number to the wavelength of the disturbance, and this has the same shape as the Darcy–Benard problem, namely that it has one well-defined minimum and that Ra tends to infinity as the wavelength of the vortex tends either to zero or to infinity; for details see Rees et al. [37]. The critical Rayleigh number and wavenumber are given by

$$Ra^{1/2}\tan\alpha = 16.8469 \quad k_c = 0.5166 \tag{9.96}$$

From this we see that the critical Rayleigh number becomes infinite as the surface approaches the vertical, and therefore we conclude that the ADP conditions described in Section 9.3 are also realizable in practice from the point of view of stability. Some fully nonlinear computations are also presented in Rees et al. [37].

A very detailed analysis of the weakly nonlinear convection in a Darcy–Benard problem is given in Rees et al. [15]. When viscous dissipation is absent then convection arises when the Darcy–Rayleigh number exceeds $4\pi^2$. Initially, convection sets in as a set of parallel rolls when the layer is of infinite horizontal extent. When viscous dissipation is present the temperature profile within the layer loses its up/down symmetry when convection occurs, and this causes hexagonal cells to arise. This is because the lack of symmetry allows two rolls, whose axes are at 60° to one another, to interact and reinforce a roll at 60° to each of them, thus providing the hexagonal pattern. Hexagonal convection is subcritical and appears at Rayleigh numbers below $4\pi^2$. However, when Ra is sufficiently above $4\pi^2$, the rolls are re-established as the preferred pattern of convection. When Forchheimer terms are included,

then the range of Rayleigh numbers over which hexagons exist and are stable decreases, and they are eventually extinguished. A similar qualitative result has been shown when the layer is tilted at increasing angles from the horizontal, although there are two main orientations of hexagonal solutions in this case. The rolls that form when hexagons are destabilized are longitudinal rolls and may be regarded as streamwise vortices like those considered in Rees et al. [37].

9.7 Research Opportunities

We close this chapter with some proposals for research opportunities.

- While the form of the viscous dissipation term for Darcy and Darcy–Forchheimer flows are well established, there remain some differences over the correct form when boundary effects are significant. Till date there exists no REV model of viscous dissipation, nor are there any detailed computations in periodically structured porous media at small length-scales.
- As far as we are aware, free, forced, and mixed convective backward boundary-layer flows, where the edge ($x = 0$) of the semi-infinite vertical plate is (not a leading edge but) a trailing edge, has not yet been investigated in the literature.
- Numerical (perturbation) solutions to the mixed convection problem for small values of the Gebhart number have only been discussed here for the two "aiding" cases of Darcy flow. The discussion of the Darcy–Forchheimer case is still open. In addition, the investigation of the two "opposing cases," and for both the Darcy and the Darcy–Forchheimer cases, is also an open problem.
- Currently no published studies on strongly nonlinear free convection in cavities and in the presence of viscous dissipation exist. Given our observations, here, regarding the manner in which up/down symmetry is broken, it is very likely that novel qualitative phenomena arise in cavities with heating from below or from sidewall.

Nomenclature

ADP	asymptotic dissipation profile
Br	Brinkman number
c_{fp}	coefficient of Forchheimer term
C	Forchheimer coefficient
c_{p}	specific heat

Da	Darcy number
Ec	Eckert number
f	reduced streamfunction
$\underline{F}$	drag force
g	gravity
Ge	Gebhart number
k	thermal conductivity of the porous medium
K	permeability
L	representative length
Nu	Nusselt number
$\underline{\underline{K}}$	permeability tensor
Pe	Péclet number
Pr	Prandtl number
q'''	volumetric rate of heat production
Q	dimensionless heat flux
$Ra,\ R$	Darcy–Rayleigh number
Re	Reynolds number
REV	representative elementary volume
s_g	projection of $g/\|g\|$ on the x-axis
s_T	$\mathrm{sgn}(T_\mathrm{w} - T_\infty)$
T	temperature
u, v, w	velocities in the x-, y-, and z-directions, respectively
U	representative velocity
x, y, z	Cartesian coordinates
Y	dimensionless y-coordinate

Greek letters

α	thermal diffusivity/inclination angle
β	thermal expansion coefficient
ΔT	representative temperature difference
ε	local Gebhart number
η	similarity variable
θ	scaled temperature
μ	dynamic viscosity
$\tilde{\mu}$	effective viscosity
ν	kinematic viscosity
ξ	dimensionless x-coordinate
ρ	fluid density
τ	scaled x-coordinate
Φ	heat source term
ψ	streamfunction

Subscripts

clear	clear fluid
Darcy	porous medium

ref	reference conditions
w	wall or surface condition
x	local quantity
∞	ambient conditions
δ	boundary-layer thickness

References

1. B. Gebhart. Effects of viscous dissipation in natural convection. *J. Fluid Mech.* 14: 225–232, 1962.
2. H.I. Ene and E. Sanchez-Palencia. On thermal equation for flow in porous media. *Int. J. Eng. Sci.* 20: 623–630, 1982.
3. A. Bejan. *Convection Heat Transfer*, 2nd edn. New York: John Wiley & Sons, 1995.
4. A. Nakayama and I. Pop. Free convection over a non-isothermal body in a porous medium with viscous dissipation. *Int. Comm. Heat Mass Transfer* 16: 173–180, 1989.
5. D.B. Ingham, I. Pop, and P. Cheng. Combined free and forced convection in a porous medium between two vertical walls with viscous dissipation. *Transp. Porous Media* 5: 381–398, 1990.
6. E. Magyari, I. Pop, and B. Keller. Effect of viscous dissipation on the Darcy forced convection flow past a plane surface. *J. Porous Media* 6: 111–112, 2003.
7. B. Tashtoush. Analytical solution for the effect of viscous dissipation on mixed convection in saturated porous media. *Transp. Porous Media* 41: 197–209, 2000.
8. P.V.S.N. Murthy. Effect of viscous dissipation on mixed convection in a non-Darcy porous medium. *J. Porous Media* 4: 23–32, 2001.
9. E. Magyari, I. Pop, and B. Keller. Comment on "analytical solution for the effect of viscous dissipation on mixed convection in saturated porous media." *Transp. Porous Media* 53: 367–369, 2003.
10. B. Tashtoush. Reply to comments on "analytical solution for the effect of viscous dissipation on mixed convection in saturated porous media." *Transp. Porous Media* 41: 197–209, 2000 and 53: 371–372, 2003.
11. D.A. Nield. Comments on "Comments on 'analytical solution for the effect of viscous dissipation on mixed convection in saturated porous media' ." *Transp. Porous Media* 55: 117–118, 2004.
12. B. Gebhart and J. Mollendorf. Viscous dissipation in external natural convection flows. *J. Fluid Mech.* 38: 97–107, 1969.
13. D.A. Nield. Resolution of a paradox involving viscous dissipation and nonlinear drag in a porous medium. *Transp. Porous Media* 41: 349–357, 2000.
14. E. Magyari and B. Keller. The opposing effect of viscous dissipation allows for a parallel free convection boundary-layer flow along a cold vertical flat plate. *Transp. Porous Media* 51: 227–230, 2003.
15. D.A.S. Rees, E. Magyari, and B. Keller. Hexagonal cell formation in a Darcy–Benard convection with viscous dissipation and its modification by form drag and layer inclination. Submitted for publication, 2004.
16. D.A. Nield. Modelling fluid flow in saturated porous media and at interfaces. In: D.B. Ingham and I. Pop, eds., *Transport Phenomena in Porous Media II*. London: Pergamon, 2002, pp. 1–19.

AQ: Please update ref[15]

17. D.A. Nield and A. Bejan. *Convection in Porous Media*, 2nd edn. New York: Springer-Verlag, 1999.
18. C.C. Mei and J.L. Auriault. The effect of weak inertia on flow through a porous medium. *J. Fluid Mech.* 647–663, 1991.
19. J.L. Lage, B.V. Antohe, and D.A. Nield. Two types of nonlinear pressure-drop versus flow-rate relation observed for saturated porous media. *ASME J. Fluids Eng.* 119: 701–706, 1997.
20. A.K. Al-Hadhrami, L. Elliott, and D.B. Ingham. A new model for viscous dissipation across a range of permeability values. *Transp. Porous Media* 53: 117–122, 2003.
21. P. Cheng and W.J. Minkowycz. Free convection about a vertical flat plate embedded in a porous medium with application to heat transfer from a dike. *J. Geophys. Res.* 82: 2040–2044, 1977.
22. S. Goldstein. On backward boundary layers and flow in converging passages. *J. Fluid Mech.* 21: 33–45, 1965.
23. D.A.S. Rees, E. Magyari, and B. Keller. The development of the asymptotic viscous dissipation profile in a vertical free convective boundary layer flow in a porous medium. *Transp. Porous Media* 53: 347–355, 2003.
24. P.V.S.N. Murthy and P. Singh. Effect of viscous dissipation on a non-Darcy natural convection regime. *Int. J. Heat Mass Transfer* 40: 1251–1260, 1997.
25. P.V.S.N. Murthy. Thermal dispersion and viscous dissipation effects on non-Darcy mixed convection in a fluid saturated porous medium. *Heat Mass Transfer* 33: 295–300, 1998.
26. H.S. Takhar, V.M. Soundalgekar, and A.S. Gupta. Mixed convection of an incompressible viscous fluid in a porous medium past a hot vertical plate. *Int. J. Non-linear Mech.* 25: 723–728, 1990.
27. M. Kumari and G. Nath. Simultaneous heat and mass transfer under unsteady mixed convection along a vertical slender cylinder embedded in a porous medium. *Warme Stoffubertragung* 28: 97–105, 1993.
28. K.A. Yih. Viscous and Joule heating effects on non-Darcy MHS natural convection flow over a permeable sphere in porous media with internal heat generation. *Int. Comm. Heat Mass Transfer* 27: 591–600, 2000.
29. M.F. El-Amin. Combined effect of viscous dissipation and Joule heating on MHD forced convection over a non-isothermal horizontal cylinder embedded in a fluid saturated porous medium. *J. Magnetism Magn. Mater.* 263: 337–343, 2003.
30. C. Israel-Cookey, A. Ogulu, and V.B. Omubo-Pepple. Influence of viscous dissipation and radiation on unsteady MHD free-convection flow past an infinite heated vertical plate in a porous medium with time-dependent suction. *Int. J. Heat Mass Transfer* 46: 2305–2311, 2003.
31. M. Kumari, H.S. Takhar, and G. Nath. Mixed convection flow over a vertical wedge embedded in a highly porous medium. *Heat Mass Transfer* 37: 139–146, 2001.
32. H.S. Carslaw and J.C. Jaeger. *Conduction of Heat in Solids*. Oxford: Clarendon Press, 1995.
33. D.A. Nield, A.V. Kuznetsov and Ming Xiong. Thermally developing forced convection in a porous medium: parallel plate with walls at uniform temperature, with axial conduction and viscous dissipation effects. *Int. J. Heat Mass Transfer* 46: 643–651, 2003.

AQ: Please provide the vol. number for ref. 18

34. A.V. Kuznetsov, Ming Xiong, and D.A. Nield. Thermally developing forced convection in a porous medium: circular duct with walls at uniform temperature, with axial conduction and viscous dissipation effects. *Transp. Porous Media* 53: 331–345, 2003.
35. A.K. Al-Hadhrami, L. Elliott, and D.B. Ingham. Combined free and forced convection in vertical channels of porous media. *Transp. Porous Media* 49: 265–289, 2002.
36. D.A.S. Rees. Stability analysis of Darcy–Benard convection. Lecture notes from *Summer School on Porous Media, Neptun, Constanta, Romania, July 2001*. (Notes available from the author.)
37. D.A.S. Rees, E. Magyari, and B. Keller. Vortex instability of the asymptotic dissipation profile in a porous medium. Submitted for publication, 2004.

AQ: Please update for ref [37]